Final DOE Project Report

Doug Crawford-Brown and Marc Serre (6-1-06)

This project focused on extension of a generalized state-vector model developed by Crawford-Brown and Hofmann (1-4). The model incorporates phenomena such as DNA damage and repair, intercellular communication mechanisms, both spontaneous and radiation-induced cell death and cell division, to predict cellular transformation following exposure to ionizing radiation. Additionally, this model may be simulated over time periods that correspond to the temporal scale of biological mechanisms.

The state-vector model has been shown to generally reproduce transformation frequency patterns for in vitro studies (2), but still significantly underpredicted *in vivo* cancer incidence data at the higher doses for high-LET radiations when biologically realistic rate constants for cell killing are included (1). Mebust et al. (1) claimed that one reason for this underprediction might be that the model's ability to fit the in vitro data is due in part to compensating errors that only reveal themselves when the more complex in vivo and epidemiological data are considered. This implies that the original in vitro model may be based on incomplete assumptions regarding the underlying biological mechanisms.

The present research considered this explanation for the case of low LET radiation. An extension of the in vitro state-vector model was tested that includes additional biological mechanisms in order to improve model predictions with respect to dose-response data on in vitro oncogenic transformation of C3H10T1/2 mouse fibroblast cells exposed to acute doses of X-radiation (5). These data display a plateau of transformation frequency per surviving cell in the X-ray dose range of 0.1 to 1 Gy, with an increase in transformation frequency at higher acute doses. To reproduce these trends in the data, additional biological processes were formulated mathematically and incorporated into the existing model as parameters whose values could be adjusted and tested by an optimization method (genetic algorithm). The model extension presented here includes many of the same biological phenomena as the original state-vector model, though some mathematical representations of these mechanisms have been adjusted and new pathways in which these events occur have been included. In addition to these original processes, this state-vector model extension incorporates: (i) pre-irradiation background transformation, (ii) the bystander effect on cell killing and (iii) an explicit representation for compensatory proliferation. These experimentally recognized biological mechanisms are established as important processes within carcinogenesis and their ability to improve model predictions should be explored.

The first additional biological mechanism considered in the present study was background transformation of cells, or transformations that occur in the absence of radiation from the experiment. They are considered to be produced randomly in cells (6), and without respect to any advantage that they might offer to the cell. These background transformations may originate from biological processes such as DNA replication errors, recombination errors and repair errors. Additionally, spontaneous DNA damage may be caused by the metabolic production of mutagenic byproducts of normal metabolism, the

intrinsic instability of DNA, oxygen toxicity and DNA turnover (7). Background transformation frequency measurements have been reported for many in vitro experiments (8-10).

The second biological mechanism incorporated into the extended model, compensatory proliferation, is governed by intercellular communication processes. Intercellular communication facilitates the homeostatic control of a population of cells, maintaining a balance between the number of cells dying and the number of cells dividing. The ability of cells to communicate via gap junctions allows both excitable and non-excitable cells to synchronize their biological functions and to cooperate metabolically (11). This gap junctional intercellular communication permits for contact inhibition to act as a growth control in normal cells. If gap junction channels are disrupted, single cells can escape these normal regulatory signals (12). Gap junctional intercellular communication is frequently observed to be reduced in neoplastic and carcinogen-treated cells (13). Thus, transformed and malignant cells commonly lack contact inhibition.

The last biological mechanism incorporated into the present model was a bystander cell-killing effect. Scientific understanding of the bystander effect is still preliminary (14-16). A long-standing theory of radiation biology was that most effects induced by ionizing radiation are the result of DNA damage arising from direct interactions between radiation and the cell nuclei (17). As early as the 1940's (18) though, studies arose suggesting that this concept may need modifications to account for the indirect effects of ionizing radiation. More recently in the 1990's, sufficient evidence accumulated to reveal that many important cancer-related cellular effects of ionizing radiation occur in the absence of direct irradiation. The term 'bystander effect' is used to describe such phenomena and has become loosely defined as the induction of biological effects in cells that are not directly traversed by a charged particle (18).

The bystander effect may be induced in a non-irradiated cell by secretion of soluble transmissible factors from a neighboring irradiated cell or by direct cell-to-cell communication through gap junctional intercellular communication (19). Further, the bystander phenomena seems to be more prevalent at low doses of radiation, effectively 'saturating' with increasing dose, where effects tend to occur in a dose-dependent manner (20-23).

The extended state-vector model used in the present study consists of seven states through which cells must pass on their way to tumor formation. States 0 through 4 denote the initiation phase of the model, state 5 depicts the irreversible promotion stage and state 6 represents a fully progressed cell. Cells in all states may replenish themselves through mitosis and may die due to both background and radiation-induced cell death. First-order transition rate constants that represent biological events control the movement of cells through the model. These transitions may contain both background and radiation induced components. Reproduction of the in vitro transformation frequency data considered for this research only involves the simulation of initiation mechanisms, reducing the model to the first five states (0 through 4). Figure 1 shows a schematic representation of the initiation portion of this extended state-vector model. Mathematical details are provided

in references 1-4; the revised model is described fully in a recently submitted paper (Crawford-Brown, Fleischman, L. and Hofmann, W., Application of a Generalized State-Vector Model for Radiation-Induced Cellular Transformation to in vitro Irradiation Cells by Acute Dose of X-Rays, Radiation Research, in revision) and in a recently accepted paper (Schollenberger, H., Mitchell, R., Crawford-Brown, D. and Hofmann, W., Detrimental Bystander Effects, Low-Dose Hyper-Radiosensitivity and Apoptosis-Mediated Protection: A Model Approach, accepted in Radiation Research, 2006).

Allowing Ni(t) to be the number of cells in State i at any time t, the state of the cellular community at this time can be represented by the vector:

$$[N_0(t), N_1(t), N_2(t), N_3(t), N_4(t)]$$

$$\text{where } N_1(t) = N_{1s}(t) + N_{1ns}(t) . \tag{1}$$

Then, the total cell count at any time, t, is:

$$N_T(t) = N_o(t) + N_1(t) + N_2(t) + N_3(t) + N_4(t) . \tag{2}$$

Furthermore, the transformation frequency per surviving cell (fraction of state 4 cells), the model calculation of interest in the present research, is calculated by:

$$f_4(t) = \frac{N_4(t)}{N_T(t)} . \tag{3}$$

Six first-order differential equations may describe the movement of these cells through the states in the model. All rate constants contain both background and radiation-induced components. In previous publications, there was a background rate constant for the interaction between breaks entirely separate from the radiation-induced rate constant. In the present research, this assumption was replaced by a more biologically plausible sequence of assumptions: that the rate of interaction of breaks is proportional to the spatial density of such breaks; that this spatial density is proportional to the rate of production of such breaks; and that this rate of production is proportional to the dose-rate This change had little effect on the predictions of the model. Resulting parameter values obtained from the optimizations are shown in the table below.

Parameters Used in the Model Equations

Rate Constant	Value and Units	Reference
k01sb	30 per day	Koteckia
k01nsb	69.9 per day	Mebust et al. (1)
k01nsr	101.8 per Gy	Mebust et al. (1)
k01sr	0 per Gy	Crawford-Brown and Hofmann (2-3)b
k23r	4 per Gy	Crawford-Brown and Hofmann (2)

k23b	10-3 Gy/year	Mean low-LET background dose-rate
krs	80 per day	Mebust et al. (1)
krns	3.12 per day	Mebust et al. (1)
kdr	1.67 per Gy	Crawford-Brown and Hofmann (4)
kdb	0.01 per day	Mebust et al. (1)
km	1 per day	Crawford-Brown and Hofmann (3)c
P4	5x10-4 per day	Crawford-Brown and Hofmann (3)
kmi	0.9995 per day	Crawford-Brown and Hofmann (3)
DR (dose < 1 Gy)	0.32 Gy/min	Miller et al. (5)
DR (dose ≥ 1 Gy)	1.8 Gy/min	Miller et al. (5)

a M. R. Kotecki, Application of a state-vector model for radiation carcinogenesis to exposures of radon progeny in the lung: test of the coherence between in vitro and in vivo models. Dissertation, Department of Environmental Sciences and Engineering, University of North Carolina at Chapel Hill, 1998.

bThe value of this parameter is too small to be determined from the existing data; it is set to 0 here in the absence of more definitive data on which it might be estimated- the effect is unlikely to be significant.

cUntil confluence, then equal to rate constant for cell death.

The present research solved the system of differential equations with a numerical approximation. The software package MATLAB was chosen for its high-performance capacity for numerical computations and built-in numerical ordinary differential equation solving functions. Since the extended state-vector model contains stiff equations, the solver 'ode15s' was chosen because it could manage this type of a system. The optimization was implemented as follows: Given the independent variable of acute X-ray dose, denoted as di, for i=1, 2,…9, the transformation frequency calculated by the extended state-vector model for dose i is f(di). Also, allow yi to signify the Miller et al. (5) transformation frequency measurement at dose i. Then the summed relative error may be expressed:

$$\sum_{i=1}^{9} \left| \frac{y_i - f(d_i)}{y_i} \right| \tag{4}$$

Summed relative errors were calculated for a 5-dimensional space of parameter combinations and a minimum value was found in this 5-dimensional matrix. The parameter value combination that corresponded to this minimum summed relative error value was chosen as the optimal unknown parameter combination.

The present research then incorporated the three phenomena of background transformation, compensatory proliferation and bystander cell-killing response into the state-vector model through the addition of five new parameters:

1. Background transformation frequency

2. Cell division rate during compensatory proliferation (a multiplicative factor applied to the normal mitotic rate), caused by removal of contact inhibition
3. Number of surrounding inactivated cells required for the removal of contact inhibition from an initiated cell,
4. Time until compensatory proliferation ceases due to the growth of new cells that restore intercellular communication following acute irradiations
5. Bystander cell-killing response

These unknown parameters were incorporated into the model with the objectives of retaining the original state-vector model structure and plausibly translating the new biological mechanisms involved into mathematical expressions within the state-vector model. The equations necessary for unknown parameter incorporation and their location in the state-vector model structure follow in the subsequent paragraphs.

Transformation frequency per surviving cell calculations using the extended state-vector model may be compared to the Miller et al. (5) in vitro transformation data in log-log graphical form. The figure below displays model predictions of the extended state-vector model that includes the five new parameters. As these optimal values were determined from a biologically plausible range, each value is consistent with experimental measurements in the current literature. Extension of the model predictions to very low doses indicate that the transformation frequencies remain level between 0 and 100 mGy with values close to the background rate.

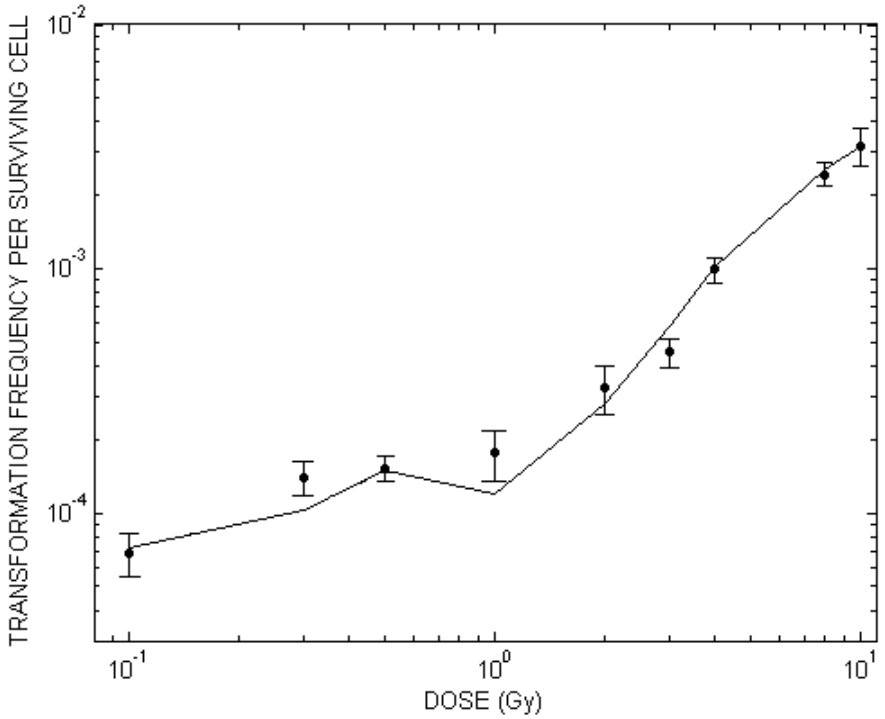

FIGURE: Transformation frequency per surviving cell for X-rays irradiated acutely (closed circles). The solid line is the result of calculations using the model.

This 5-parameter model tends to slightly underpredict transformation frequencies at doses of 0.3 and 1 Gy, but the low dose plateau in the data is reproduced fairly well and the

marked increase at doses above 1 Gy is predicted almost perfectly. These predictions were optimized by a bystander effect parameter value of 0.35, which represents a protective bystander cell-killing response. Therefore, with respect to the data, it may be concluded that the extended state-vector model has a reasonably good ability to explain and predict in vitro phenomena of cellular transformation by X-radiation.

Further analysis of the extended state-vector model assessed model sensitivity to the individual parameters. Two forms of sensitivity were considered: local and global. In the global sensitivity analysis, a single parameter was adjusted upwards and downwards, and then the complete optimization routine run to determine best fits for the adjustable parameters under each selection of the adjusted parameter. The numerical values of the other parameters, therefore, will vary slightly between the different runs of the adjusted parameter. In the local sensitivity analysis, best fitting values were obtained for all parameters in the model, and then only the adjusted parameter was changed to determine the local sensitivity of the model to that change. Both forms of sensitivity analysis are informative and so are included here. Representative results is shown in the figures above and below.. Model sensitivity calculations for the kdmult parameter, illustrated graphically in Figure 4, demonstrate that the model is sensitive to the protective bystander response on cell-killing only at the higher radiation doses (above 1 Gy). The solid lines with closed circles are the result of optimal model calculations, the dashed lines demonstrate model calculations with variation in the parameters.

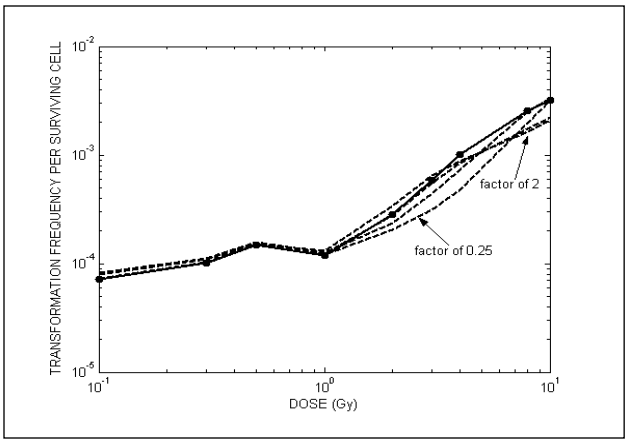

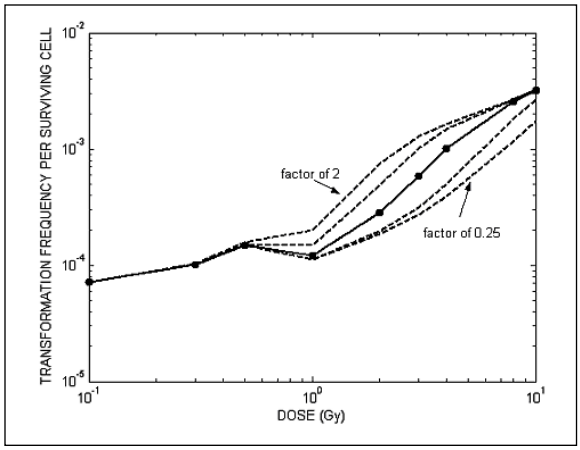

The results of the present study demonstrate that the extended state-vector model is predictive of observed in vitro results obtained with X-rays. The optimal parameter value calculated for the bystander cell-killing effect was less than 1, suggesting that the bystander effect acts in protecting against cell-killing. While the protective role of bystander effects has been observed experimentally, this is generally detected at very low doses of radiation. Conversely, the present research suggests that the protective bystander effect on cell-killing may be more effective at higher doses, above 1 Gy (Figure 3).

A comment is warranted here on the continued use of the Miller et al data (5), which are now more than two decades old (several colleagues and reviewers commented on this). Newer data, such as those developed by Azzam et al (24,25), indicate an adaptive response following exposure to pre-conditioning doses, which can reduce the transformation frequency at low doses below those of the controls. These data at least suggest that the low-dose region may be characterized by an initial decrease in transformation frequency followed by a rise, rather than the slight rise followed by a plateau and subsequent sharper rise evident in the figures above, although they are not as detailed in the selection of doses as the dosing regime used in the data from Miller at al (5). The current model at least suggests such a decrease, although it predicts it to be at approximately 1 Gy, and to be preceded at lower doses by a slight elevation in transformation frequency per surviving cell. This feature of the model remains even when adaptive response is formally included in the model.

We have chosen to remain with the Miller et al (5) data because (i) the methodology used in generating the data remains sound, (ii) the study provides data under both acute and split dose conditions, a feature essential in establishing some of the rate constants in previous developments of the model (2,3) and (iii) our goal is to explore how incorporation of some new biological features and mathematical formulations in the model affects the behavior of that model, which would be complicated by switching both the model and the data used to develop parameters for the model.

A natural next step in the research was to begin to incorporate adaptive response mechanisms into this expanded model, and preliminary research has now been completed on that (published in the Schollenberger et al 2006 paper mentioned previously). That study incorporated a variety of low-dose effects such as detrimental by-stander effects, low-dose hyper-radiosensitivity, (the underlying biological mechanism is essentially an absence of DSB repair at low doses due to the continued attempts of damaged G2 cells to progress through the cell cycle), and apoptosis-mediated protective bystander effects. This component of the research program demonstrated that:

- The SVM can be equipped with features of detrimental and protective bystander effects and with low-dose HRS with a reasonably low number of free parameters. The model was successfully fitted to appropriate data sets.

- Within the SVM the chosen approach to fit the Nagasawa and Little data is equivalent to bystander-induced promotion of initiated cells. The control and high dose data for the X-ray sensitive xrs-5 cells were fitted with only one free parameter that allowed for the impairment of DSB repair in this cell line.

- Some data sets on in vitro chromosome aberrations after α-particle exposure might exhibit an area of hyper-radiosensitivity at low doses previously unaccounted for.

- The concept of a bystander-induced apoptosis-mediated protective effect was applied to successfully explain in vitro data, which showed that low-dose rate γ-irradiation

reduced the neoplastic transformation frequency below the level of spontaneous transformation. It was found that the magnitude of the protective effect is strongly dependent on PAM duration.

- New experiments are needed that investigate the potential of low doses (< 200 mGy) of low-LET radiation to induce apoptosis. The requested studies should investigate the time dependence of apoptosis induction for at least three to four weeks post-exposure.

- The importance of adaptive responses with respect to a reduction of the background neoplastic transformation frequency at low doses and low dose rates is emphasized.

The following acknowledgement was provided for each publication:

This research was supported by the Office of Science (BER), U.S. Department of Energy, Grant Number DE-FG02-03ER63673.

REFERENCES CITED IN THIS PROJECT REPORT

1. M. Mebust, D. J. Crawford-Brown, W. Hofmann and H. Schöllnberger, Testing extrapolation of a biologically-based exposure-response model from in vitro to in vivo to human epidemiological conditions. Regul. Toxicol. Pharmacol. 35, 72-79 (2002).
2. D. J. Crawford-Brown and W. Hofmann, A generalized state-vector model for radiation-induced cellular transformation. Intl. J. Radiat. Biol. 57, 407-423 (1990).
3. D. J. Crawford-Brown and W. Hofmann, Extension of a generalized state-vector model of radiation carcinogenesis to consideration of dose rate. Math. Biosci. 115, 123-144 (1993).
4. D. J. Crawford-Brown and W. Hofmann, The testing of radiobiological models of radon carcinogenesis needed for in vitro to in vivo extrapolations. Environ. Int. 22 (Suppl. 1), S985-S994 (1996).
5. R. C. Miller, E. J. Hall and H. H. Rossi, Oncogenic transformation of mammalian cells in vitro with split doses of x-rays. Proc. Natl. Acad. Sci. 76, 5755-5758 (1979).
6. L. Natarajan, C. C. Berry and C. Gasche, Estimation of spontaneous mutation rates. Biometrics 59, 555-561 (2003).
7. K. C. Smith, Spontaneous mutagenesis: Experimental, genetic and other factors. Mutat. Res. 277, 139-162 (1992).
8. D. A. Lewis, B. M. Mayhugh, Y. Qin, K. Trott and M. S. Mendonca, Production of delayed death and neoplastic transformation in CGL1 cells by radiation-induced bystander effects. Radiat. Res. 156, 251-258 (2001).
9. J. L. Redpath and R. J. Antoniono, Induction of an adaptive response against spontaneous neoplastic transformation in vitro by low-dose gamma radiation. Radiat. Res. 149, 517-520 (1998).
10. J. L. Redpath, D. Liang, T. H. Taylor, C. Christie and E. Elmore, The shape of the dose-response curve for radiation-induced neoplastic transformation in vitro:

Evidence for an adaptive response against neoplastic transformation at low doses of low-LET radiation. Radiat. Res. 156, 700-707 (2001).
11. J. E. Trosko, C. C. Chang and B. V. Madhukar, Modulation of intercellular communication and uncontrolled growth. Radiat. Res. 123, 241-251 (1990).
12. M. R. Wilson, T. W. Close and J. E. Trosko, Cell population dynamics (apoptosis, mitosis, and cell-cell communication) during disruption of homeostasis. Exp/ Cell Res. 254, 257-268 (2000).
13. J. E. Trosko and R. J. Ruch, Cell-cell communication in carcinogenesis. Front. Biosci. 3, d208-236 (1998).
14. O. V. Belyakov, M. Folkard, C. Mothersill, K. M. Prise and B. D. Michael, A proliferation-dependent bystander effect in primary porcine and human urothelial explants in response to targeted irradiation. Br. J. Cancer. 88, 767-774 (2003).
15. D. J. Brenner, J. B. Little and R. K. Sachs, The bystander effect in radiation oncogenesis: II, A quantitative model. Radiat. Res. 155, 402-408 (2001).
16. C. Mothersill and C. Seymour, Radiation-induced bystander effects: Past history and future directions. Radiat. Res. 155, 759-767 (2001).
17. R. Iyer and B. E. Lehnert, Effects of ionizing radiation in targeted and nontargeted cells. Arch. Biochem. Biophys. 376, 14-25 (2000).
18. E. J. Hall, The bystander effect. Health Phys. 85, 31-35 (2003).
19. B. Wang, H. Ohyama, Y. Shang, K. Fujita, K. Tanaka, T. Nakajima, S. Aizawa, O. Yukawa and I. Hayata, Adaptive response in embryogenesis: IV. Protective and detrimental bystander effects induced by X radiation in cultured limb bud cells of fetal mice. Radiat. Res. 161, 9-16 (2004).
20. F. M. Lyng, C. B. Seymour and C. Mothersill, Production of a signal by irradiated cells which leads to a response in unirradiated cells characteristic of initiation of apoptosis. Br. J. Cancer 83, 1223-1230 (2000).
21. F. M. Lyng, C. B. Seymour and C. Mothersill, Initiation of apoptosis in cells exposed to medium from the progeny of irradiated cells: A possible mechanism for bystander-induced genomic instability. Radiat. Res. 157, 365-370 (2002).
22. C. Mothersill, T. D. Stamato, M. L. Perez, R. Cummins, R. Mooney and C. B. Seymour, Involvement of energy metabolism in the production of 'bystander effects' by radiation. Br. J. Cancer 82, 1740-1746 (2000).
23. C. B. Seymour and C. Mothersill, Relative contribution of bystander and targeted cell killing to the low-dose region of the radiation dose-response curve. Radiat. Res. 153, 508-511 (2000).
24. E. Azzam, S. de Toledo, G. Raaphost and R. Mitchel, Low dose ionizing radiation decreases the frequency of neoplastic transformation to a level below the spontaneous rate in C3H10T1/2 cells, Radiat. Res. 146, 369-373 (1996).
25. E. Azzam, G. Raaphost and R. Mitchel, Radiation-induced adaptive response for protection against micronucleus formation and neoplastic transformation in C3H10T1/2 mouse embryo cells, Radiat. Res. 138, S28-S31 (1994)